INSTITUTE OF PHYSICS PUBLISHING JOURNAL OF PHYSICS B: ATOMIC, MOLECULAR AND OPTICAL PHYSICS

J. Phys. B: At. Mol. Opt. Phys. **34** (2001) 3669–3678 PII: S0953-4075(01)23490-7

K-shell photoionization of CO and N_2: is there a link between the photoelectron angular distribution and the molecular decay dynamics?

Th Weber[1], O Jagutzki[1], M Hattass[1], A Staudte[1,2], A Nauert[1], L Schmidt[1], M H Prior[2], A L Landers[3], A Bräuning-Demian[1], H Bräuning[4], C L Cocke[5], T Osipov[5], I Ali[5], R Díez Muiño[2], D Rolles[2], F J García de Abajo[2], C S Fadley[2], M A Van Hove[2], A Cassimi[6], H Schmidt-Böcking[1] and R Dörner[7]

[1] Institut für Kernphhysik, Universität Frankfurt, August Euler Straße 6, D60486 Frankfurt, Germany
[2] Lawrence Berkeley National Laboratory, Berkeley CA 94720, USA
[3] Department of Physics, Western Michigan University, Kalamazoo, MI 49008, USA
[4] Strahlenzentrum, Leihgesterner Weg 217, D-35392 Giessen, Germany
[5] Department of Physics, Kansas State University, Manhattan, KS 66506, USA
[6] CIRIL/CEA/CNRS/ISMRA, University de Caen, Box 5133, F-14070 Caen Cedex 5, France
[7] Fakultät für Physik, University Freiburg, Hermann Herder Straße 3, D79104 Freiburg, Germany

E-mail: doerner@hsb.uni-frankfurt.de

Received 27 March 2001, in final form 10 August 2001
Published 10 September 2001
Online at stacks.iop.org/JPhysB/34/3669

Abstract

We have used COLTRIMS to measure the angular distribution of electrons released from the K-shell of N_2 and the carbon K-shell of CO by absorption of one linear polarized photon. For each ionization event which leads to two charged fragments we determine the angle of the photoelectron with respect to the fragment ion momenta. In addition we determine the charge state and energy of the molecular fragments. We find a breakdown of the axial recoil approximation for CO for kinetic energy releases below 10.2 eV, whereas for N_2 that approximation is found to be valid for all fragment energies. Furthermore, the photoelectron emission spectrum for N_2 is found to be the same for the molecular breakup channels producing N^+N^+ and N^+N^{++}.

(Some figures in this article are in colour only in the electronic version)

Photoelectron emission from an atom shows very simple angular distributions. Within the dipole approximation, they can be described by a single parameter. For photoelectron emission from a molecule, however, even within the dipole approximation, a richly structured angular distribution in the molecular fixed frame has been predicted [1–10] and observed [11–22] in

many cases. These structures result from the diffraction of the photoelectron wave in the multi-centre molecular potential. They are, in turn, a sensitive probe of molecular structure and the many-centred potentials [23].

When an inner-shell electron is emitted, the molecule fragments in most cases. To describe this process mostly a simple independent 3-step model has been invoked: first the photoelectron is released through the molecular potential. In a subsequent independent step, the Auger decay of the K-hole leads to multiple ionization and, finally, to fragmentation of the molecule. The gas phase experiments performed so far start with randomly oriented molecules and try to infer the orientation of the molecule at the instant of photoabsorption from the directions of the ionic fragments. The validity of this procedure relies on two assumptions.

- The axial recoil approximation [24], that the Auger decay and the molecular fragmentation are fast compared with the rotation of the intermediate molecular ion. Hence the fragments are emitted along the direction of the molecule at the instant of photoabsorption.
- The independence of the steps of photoelectron emission and the molecular fragmentation in the three step model. In particular, that the charge state of the fragments and the kinetic energy release (KER, which is the sum over the kinetic energies of the ionic fragments) is independent of the photoelectron emission.

The validity of the axial recoil approximation depends primarily on the lifetime of the intermediate multiply charged molecular ion. The characteristic lifetime of the K-hole is of the order of 10^{-14} s, which is much shorter than typical rotational times of 10^{-12} s. In several experiments on electron emission from fixed in space molecules the authors have restricted their data analysis to KER above a certain threshold and observed a smearing of the electron angular distributions if one includes lower energy fragments (see, e.g., [19, 20]). In this paper we have a KER resolution of below 0.1 eV, which permits a detailed check of the connection between the KER and the electron angular distributions for N_2 and CO.

The independence of the processes in the 3-step model is of importance in the two contexts of electron correlation (ground state and scattering correlation [25]) in a molecule and in the interpretation of photoionization from homonuclear molecules: a fundamental question is whether the initial-state correlation between the ionized K-electron and the rest of the electrons is strong enough to establish a link between the photoelectron ejection pattern and the subsequent decay of the molecular ion. One could speculate that the decay path of the molecular ion is already determined at the instant of the ejection of the first electron. Quantum mechanically all electrons in the initial-state wavefunction of the molecular ground state are correlated. One might hope to find traces of this correlation in a link between the K-photoabsorption and the molecular decay which goes beyond the independent 3-step model. Another possible link between the 3 steps could be provided not by initial-state correlation but by scattering correlation as the photoelectron leaves the molecule. Pavlychev [26] has shown that K-shell ionization plus excitation is an important channel in CO photoionization. The photoelectron can either excite or directly knock out a second electron on its way out of the molecule. Such electron–electron scattering is likely to depend on the direction of emission of the photoelectron in the molecular frame. These effects lead to a loss of energy of the primary electron, thus it will not contribute to the main line. This would lead to a loss of count rate in this channel at certain angles due to two-electron effects.

For homonuclear molecules, such as N_2, a second effect arises [8]. If the two centres are indistinguishable the photoelectron waves emerging from each have to be added coherently. If, however, N_2 decays after K-shell ionization asymmetrically into $N^+ + N^{++}$, one might suspect that the N^{++} has a higher likelihood to be the origin of the K-electron than the N^+ ion. In this

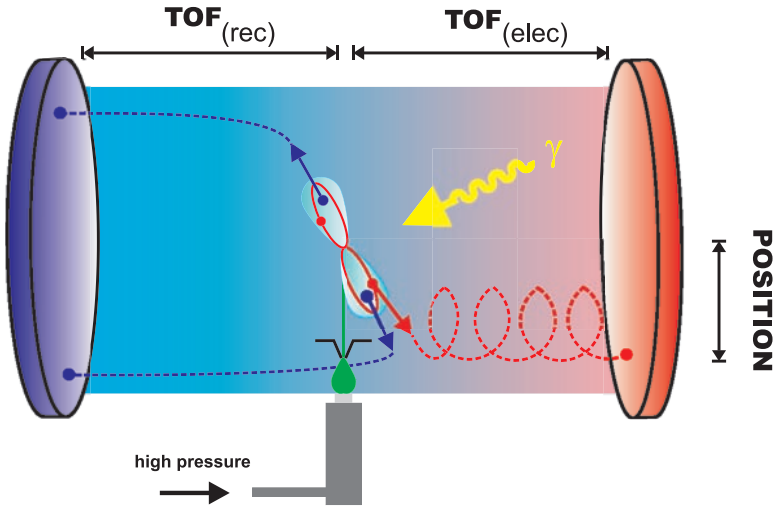

Figure 1. Schematics of the experiment, see text. A supersonic gas jet is crossed with the photon beam. The shaded area represents a superposition of an electric and magnetic field. The magnetic field result forces the electrons on cyclotron trajectories. For electron and both fragments the position of impact and the time-of-flight is measured in coincidence.

case the coherence would be partially destroyed, and the independent 3-step model would not be valid [27].

In this paper we search for a dependence of the electron angular distribution on the fragment energies and fragment channels in CO and N_2.

The experiment has been performed using COLd target recoil ion momentum spectroscopy (COLTRIMS) (see [28] for a recent review). In brief (figure 1), the beam of linear polarized photons from the bending magnet beamline BL9.3.2. at the advance light source (ALS) is crossed with a molecular supersonic beam. The photoions and photoelectrons are guided by a homogeneous electric and parallel magnetic field towards two position-sensitive micro channel plate detectors with delayline anodes (Roentdek) [29]. The fields are chosen such that electrons of up to 30 eV and ions up to 11–20 eV (depending on charge state) are collected with 4π collection solid angle. A triple coincidence is performed where we recorded only those events where two ions and one electron were detected. From the times-of-flight and the positions of impact on the detectors, the three-dimensional initial momenta of all particles are calculated in the offline analysis. For electrons of 10 eV our electron imaging yields an energy resolution of about 2 eV FWHM. This is sufficient to discriminate against satellite photoelectrons and the Auger electrons (which have several hundred eV of energy). After the full analysis there is no visible background left in the data. This effective suppression of background from random coincidences is achieved mainly because we detect both ionic fragments in coincidence and check the ionic fragment for momentum conservation. A complete description of the multidimensional momentum distributions which result from the data recorded in one experiment of this kind is beyond the scope of the present paper. Here we concentrate on the relationship between the molecular fragmentation and the electron angular distribution. Other aspects of this experiment are presented in separate publications [23, 30].

The momentum distribution and KER for N_2 after K-photoionization is shown in figure 2. The KER spectrum shows sharp peaks and is substantially different for the two fragmentation channels. Some of the lines observed from the decay of N_2^{2+} created by electron impact [31]

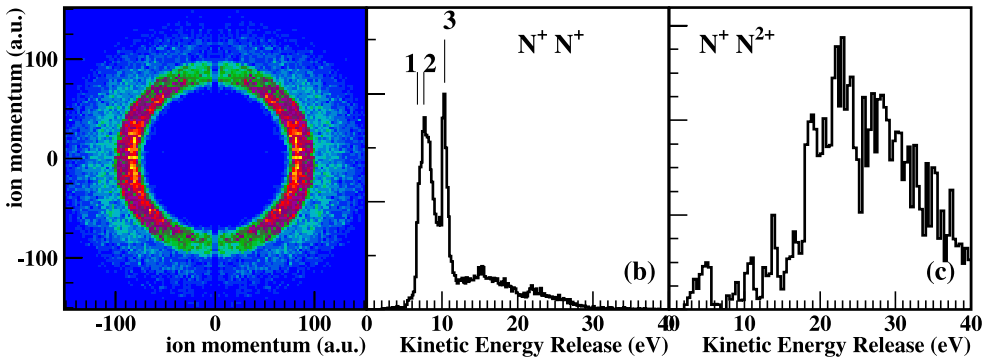

Figure 2. Fragmentation of N_2 after K-shell photoionization by 419.3 eV photons. (*a*) Momentum distribution of the N^+ ions from the $N^+ + N^+$ decay channel. The polarization is horizontal, the data are integrated over an angle of $\pm 25^\circ$ out of the plane of the figure. (*b*) Kinetic energy release (i.e. sum of both fragment energies) for the $N^+ + N^+$ decay channel. Line 1: $A^1\Pi_u \rightarrow N^+(^3P) + N^+(^3P)$, line 2: $D^3\Pi_g \rightarrow N^+(^3P) + N^+(^3P)$, line 3: $D^1\Sigma_u^+ \rightarrow N^+(^3P) + N^+(^1D)$, line positions from [31]. (*c*) KER for the $N^+ + N^{2+}$ decay channel.

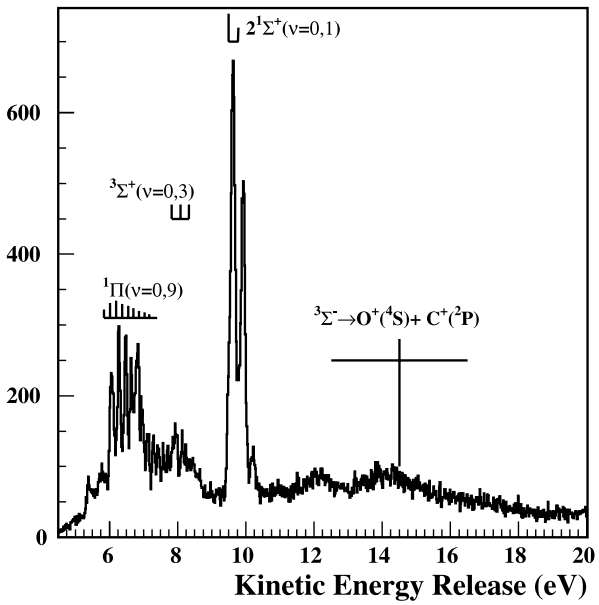

Figure 3. Kinetic energy release from CO^{2+} decaying to $C^+ + O^+$ after carbon K-shell photoionization by 306.4 eV photons. The line positions and relative strength of the vibrational resolved lines are from a high resolution measurement after electron impact by Lundqvist [33].

are indicated in figure 2(*b*). Note that these are not the only lines in the respective region. For further discussion of the KER spectra from the N_2^{2+} molecular ion we refer the reader to [32].

In figure 3 the KER from the $C^+ + O^+$ decay channel of CO after carbon K photoabsorption at the peak of the σ-shape resonance (photoelectron energy 10.4 eV) is shown. The spectrum shows very narrow peaks from vibronically excited CO^{2+}. The high resolution has been achieved by calculating the momenta of each fragment with respect to the centre of mass. This improves the experimental resolution strongly for three reasons. First the effect of thermal

motion is eliminated since the thermal velocity smears out the centre-of-mass motion, but not the momenta of the fragment with respect to the centre of mass (see [33]). Second, one of the limiting factors for the experimental resolution in the individual fragment momentum measurement is the uncertainty of the starting position within the width of the gas-jet. Since both fragments start at the same position this position uncertainty cancels out to first order if one calculates the difference of the two fragment momenta rather than their absolute value in the laboratory system. Third, the recoil momentum of the fast Auger electron does not obscure the KER measurements, since (for reasonably long lived states) this momentum is absorbed by the CO^{2+} (centre of mass) and not by one of the individual fragments. Some of the lines observed in a Doppler-free high resolution measurement with electron impact by Lundqvist *et al* [33] (see also [34–36]) are shown in figure 3. These line positions coincide with our measurements within the accuracy of our calibration. The population of the different states, however, depends on the excitation process. Hence the intensities in our KER spectrum differ from that of the electron impact experiment, where a valence electron is removed. For low-energy photon impact [32] yet another population is observed. Our KER spectrum is in qualitative agreement with a low resolution measurement by Hitchcock *et al* [36]. The broad features above 10.2 eV cannot be uniquely assigned to a particular decay channel. The width indicates that they result from purely repulsive states such as $^3\Sigma^-$ (see [37, 38] for correlation diagrams).

From our data we have also extracted carbon K-electron angular distributions for breakup of the molecule parallel to the polarization axis for several fixed KER intervals of the C^+ O^+ fragments at an electron energy of 10.4 eV which is on the shape resonance. From our coincidence measurement the KER associated with each photoelectron is known. In the analysis we can thus generate a photoelectron angular distribution which is associated with a certain chosen range of KERs. The angular distribution shows a strong dependence on the KER up to 10.2 eV (figure 4(*a*)–(*d*)). For the high fragment energies the narrow structures and deep minima, which are in good agreement with [19], show that the axial recoil approximation is well satisfied (i.e. the molecule rotates less than 10° before it decays). A rough estimate of the possible rotation can be gained by neglecting the lifetime of the molecular ion and using the measured KER to calculate the trajectory of the fragment ions. The rotation is below 5° for all of the KER lines observed here and for rotational excitation up to $l = 20$. Therefore, fragmentations which proceed via vertical transitions onto steep repulsive curves in the CO^{2+} correlation diagram do not exhibit any visible angular blurring. If the intermediate CO^{2+} state, however, has potential minima, required to produce the observed vibrational structure, there is in most cases enough time for significant rotation of the intermediate CO^{2+}. Therefore, the information about the orientation of the molecular axis at the instant of the photoelectron emission can be obscured. We can simulate this effect from our data. Events with KER >10.2 eV, where the molecule does not rotate prior to dissociation. For all these events a random rotational axis is picked in the plane perpendicular to the breakup axis. We then rotate the measured breakup axis by a random angle around the rotation axis. We point out that the data obtained in this way still have a bias for the molecular axis parallel to the polarization. This is since not all orientations of the molecule at the instant of photoionization have the same probability to be rotated into the axis of polarization. In particular, the perpendicular transition is suppressed since here the molecule can rotate around the polarization axis and in this case will never line up with this axis.

Figure 4 shows that for each KER the electron angular distribution can be fitted by summing a component, for which the axial recoil approximation is fully valid, and the randomized rotation contribution. In addition to these two extreme cases of no rotation and a random rotation there is the possibility that the lifetime is such that only partial rotation is likely.

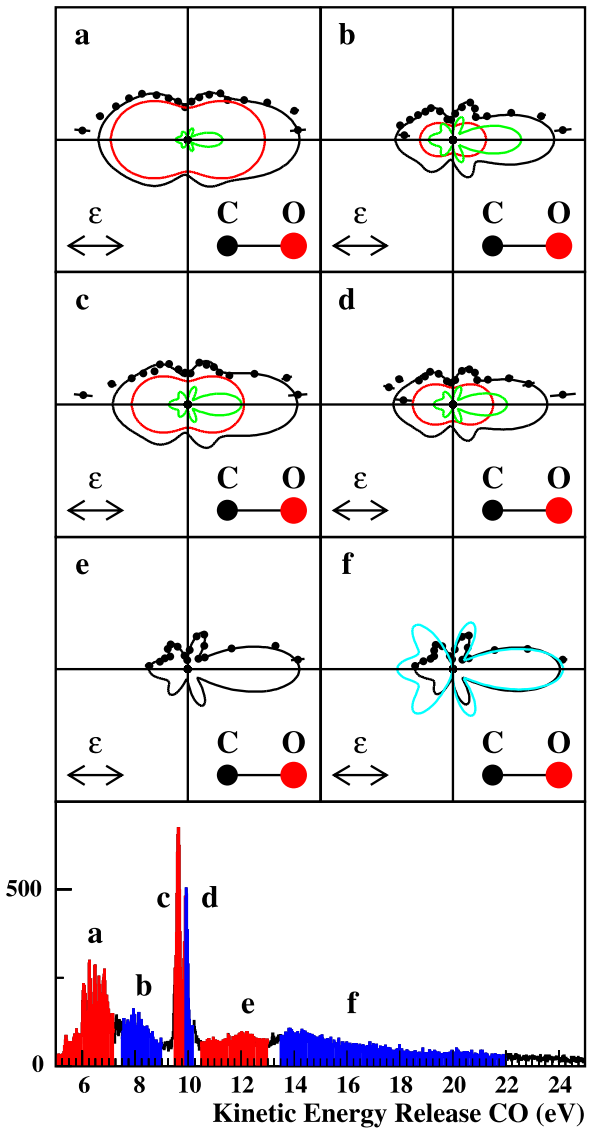

Figure 4. Angular distribution of 10.4 eV carbon K-photoelectrons ($E_\gamma = 306.4$ eV). The polarization of the linear polarized light is horizontal, the C^+ and O^+ fragments are detected parallel to the polarization (O^+ to the right). The electron and the fragments are emitted within $\pm 20^\circ$ of the plane of the figure. Each panel is arbitrarily scaled. The data shown in panels (*a*)–(*f*) are electrons coincident with regions of kinetic energy release as indicated in the lower panel. The full black curve in panel (*f*) shows a fit according to equation (1) with $l = 0, \ldots, 8$. The red (dark grey) curves show a fit to the distribution obtained by randomly rotating the molecular axis event by event in our dataset simulating a molecular rotation (see text). The black curves in panels (*a*)–(*f*) are the weighted sum of the distribution in f) and the randomized distribution, the green (light grey) and red (dark grey) curves show the contribution of each to the black curve in the respective panel. The blue (grey) curve in (*f*) shows the theoretical prediction scaled to the maximum of the distribution.

However, already the simplified assumption of only two components yields a good fit to our data. A loss of structure in the electron angular distribution for small KER has been previously reported [7, 19, 35].

The angular distribution of photoelectrons from cylindrical symmetric molecules oriented parallel to the polarization vector can, within the dipole approximation, be described by an infinite sum over Legendre polynomials (see, e.g., [10] for more details):

$$\sum_{l=0}^{\infty} A_l P_l(\cos\vartheta). \tag{1}$$

For homonuclear molecules this sum contains only the even orders.

The blue (grey) curve in figure 4(*f*) shows a theoretical calculation using multiple scattering in non-spherical potentials. Multiple scattering theory is a natural way of describing the intramolecular scattering of the electron on its way towards the detector, as shown in various classical works on the field [2–5]. However, standard multiple scattering is unable to accurately reproduce the photoelectron angular distributions at the kinetic energy range considered in this work. For this reason, we have developed a new theoretical approach based on the multiple scattering of the photoemitted electron in non-spherical space-filling potentials. Further details of the calculation and a thorough analysis of its application to the molecular photoexcitation process will be published elsewhere [39].

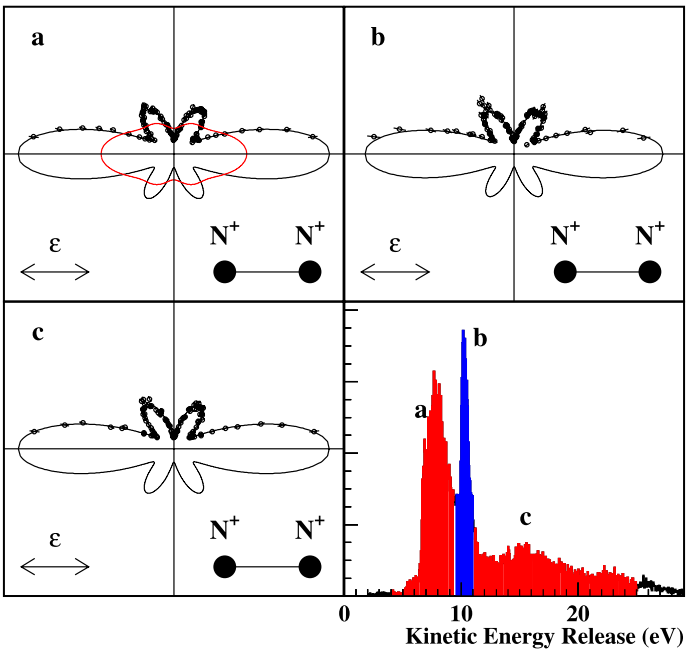

Figure 5. Angular distribution of 9.8 eV K-photoelectrons from N_2. The polarization of the linear polarized light is horizontal, the N^+N^+ fragments are detected parallel to the polarization. The electron and the fragments are emitted within $\pm 20^\circ$ of the plane of the figure. Each panel is arbitrarily scaled. The data shown in panels (*a*)–(*c*) are electrons coincident with regions of kinetic energy release as indicated in panel (*d*). The full curve is a fit of equation (1) with $l = 0, 2, 4, 6, 8$ to the sum of (*a*)–(*c*) (scaled). The red (grey) curve in panel (*a*) shows the expected distribution for random rotation of the molecular axis.

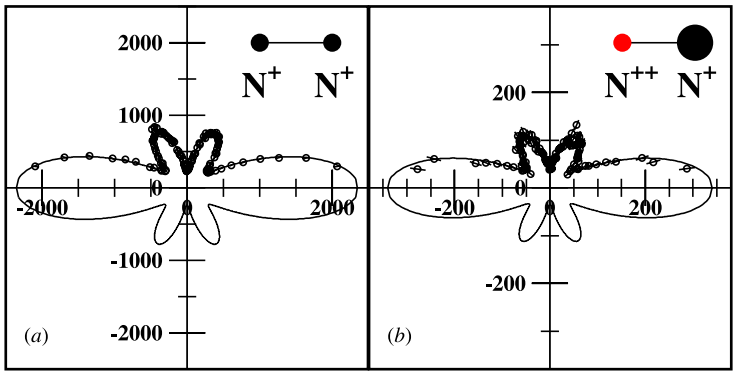

Figure 6. Angular distribution of 9.8 eV K-photoelectrons from N_2. The polarization of the linear polarized light is horizontal, the N^+ and N^{2+} fragments are detected parallel to the polarization. The electron and the fragments are emitted within $\pm 20^\circ$ of the plane of the figure. (*a*) shows electrons coincident with fragmentation to the $N^+ + N^+$ channel, (*b*) the $N^+ + N^{2+}$ decay channel. The full curve in (*a*) is a fit according to equation (1) for $l = 0, 2, 4, 6, 8$. The full curve in (*b*) is the same as in (*a*) (scaled). The data are integrated over the full range of KERs shown in figure 4.

In contrast to CO for N_2 we observe no strong dependence of the electron angular distribution for the full range of KER (figure 5). We see no indication of contributions from molecular states which live long enough to rotate significantly but short enough to be detected by our system (shorter than 50 ns). The expected distribution of a rotating N_2^{2+} intermediate state generated from our data, as outlined above, is shown for comparison in figure 5(*a*). However, states in the lifetime range discussed here have been seen in the literature [40, 41]. In most cases, however, these are high vibrational levels which do not yield a significant contribution to the KER distribution observed here.

Figure 6 shows the K-photoelectron ($E = 9.8$ eV) angular dependence of N_2 for the $N^+ + N^+$ and the $N^+ + N^{2+}$ breakup channel. The full curve is, aside from a normalization factor, the same in both figures. The question addressed by this figure is whether the asymmetric breakup destroys the coherence of the contributions from the two centres. This would have two effects: first, if the N^{2+} fragment would have a higher probability to be the location of original K-hole, the left right symmetry would be broken (as in CO see figure 4). Second, as has been pointed out by Pavlychev *et al* [8] a loss of coherence would change the ratio of the small F-wave lobes to the main lobe. Our data show no indication for such possible decoherence for the two channels investigated here.

In conclusion we have observed a strong variation of the carbon K-electron angular distribution from CO with the kinetic energy release of the fragmenting CO^{2+} and no such variation for N_2. These results show a breakdown of the axial recoil approximation in CO for KER below 10.2 eV. Below 10.2 eV the observed distributions are derivable as a sum of two distributions; one consistent with the axial recoil approximation and one from a rotating molecule. The latter arises from long lived CO^{2+} states which contribute the sharp structures to the KER spectrum below 10.2 eV (figure 4). For N_2 we observe the same symmetrical electron angular distribution for the $N^+ + N^+$ and the $N^+ + N^{2+}$ decay channel, indicating that the asymmetric decay channel does not break the coherence of the electron waves emerging from either centre. Our data for CO and N_2 do not indicate any violation of the independent 3-step model. The present experiment, however, observes the first step (the photoelectron emission) and the last step (the decay of the multiply charged molecular ion) of the process. The intermediate Auger emission remains unobserved so far. Thus we cannot conclude

that there is no link between photoelectron and Auger decay or between Auger-electron direction and fragmentation dynamics. To observe (and predict) all the details of molecular K-photoionization induced molecular fragmentation still remains a major challenge to experiment and theory. The very short time delay between photoelectron and Auger electron would, for the first time, allow for an observation of intermolecular dynamics on a few femto-second time scale. A photoelectron Auger-electron fragment-ion multiple coincidence experiment has the potential to observe not only the time dependence of nuclear motion in a molecule, but also of the much faster electronic rearrangement processes, which are the key to chemical reaction dynamics.

Acknowledgments

This work was supported by DFG, BMBF and by the US Department of Energy, Office of Science Basic Energy Sciences, Geosciences and Biosciences Division. RD acknowledges support from the Heisenbergprogramm (DFG) and the Alexander von Humboldt Foundation. ThW is grateful for support from the Graduiertenförderung des Landes Hessen. This work was supported in part by the Director, Office of Science, Office of Basic Energy Sciences and Division of Materials Sciences under US Department of Energy contract no DE-AC03-76SF00098. We thank N Cherepkov, S K Semenov, V McKoy, K Wang and A Pavlychev for helpful discussions and making their calculations available to us prior to publication. We are indebted to Uwe Becker for discussions on the coherence of electrons from homonuclear molecules. We thank the team at ALS Bl. 9.3.2. for welcoming this work at their endstation complex. We also thank the staff at ALS for extraordinary support.

References

[1] Kaplan I and Markin A 1969 *Sov. Phys. Dokl.* **14** 36
[2] Dill D 1976 *J. Chem. Phys.* **65** 1130
[3] Dill D, Siegel J and Dehmer J 1976 *J. Chem. Phys.* **65 3158**
[4] Dehmer J and Dill D 1975 *Phys. Rev. Lett.* **35** 213
[5] Dehmer J and Dill D 1976 *J. Chem. Phys.* **65** 5327
[6] Cherepkov N A and Kuznetsov V 1987 *Z. Phys.* D **7** 271
[7] Cherepkov N A, Semenov S K, Hikosaka Y, Ito K, Motoki S and Yagishita A 2000 *Phys. Rev. Lett.* **84** 250
[8] Pavlychev A A, Fominykh N G, Watanabe N, Soejima K, Shigemasa E and Yagishita A 1998 *Phys. Rev. Lett.* **81** 3623
[9] Semenov S and Cherepkov N 1998 *Chem. Phys. Lett.* **291** 375
[10] Cherepkov N A, Raseev G, Adachi J, Hikosaka Y, Ito K, Motoki S, Sano M, Soejima K and Yagishita A 2000 *J. Phys.* **33** 4213
[11] Shigemasa E, Adachi J, Oura M and Yagishita A 1995 *Phys. Rev. Lett.* **74** 359
[12] Guyon P, Golovin A, Quayle C, Vervloet V and Richard-Viard M 1996 *Phys. Rev. Lett.* **76** 600
[13] Shigemasa E, Adachi J, Soejima K, Watanabe N, Yagishita A and Cherepkov N 1998 *Phys. Rev. Lett.* **80** 1622
[14] Heiser F, Geßner O, Viefhaus J, Wieliczec K, Hentges R and Becker U 1997 *Phys. Rev. Lett.* **79** 2435
[15] Dörner R, Bräuning H, Jagutzki O, Mergel V, Achler M, Moshammer R, Feagin J, Bräuning-Demian A, Spielberger L, McGuire J *et al* 1998 *Phys. Rev. Lett.* **81** 5776
[16] Downie P and Powis I 1999 *Phys. Rev. Lett.* **82** 2864
[17] Golovin A, Heiser F, Quayle C, Morin P, Simon M, Gessner O, Guyon P and Becker U 1997 *Phys. Rev. Lett.* **79 4554**
[18] Watanabe N, Adachi J, Soejima K, Shigemasa E and Yagishita A 1997 *Phys. Rev. Lett.* **78** 4910
[19] Motoki S, Adachi J, Hikosaka Y, Ito K, Sano M, Soejima K, Yagishita G R A and Cherepkov N A 2000 *J. Phys. B: At. Mol. Phys.* **33** 4193
[20] Ito K, Adachi J, Hikosaka Y, Motoki S, Soejima K, Yagishita A, Raseev G and Cherepkov N A 2000 *Phys. Rev. Lett.* **85** 46

[21] Lafosse A, Lebech M, Brenot J C, Guyon P M, Jagutzki O, Spielberger L, Vervloet M,. Houver J C and Dowek D 2000 *Phys. Rev. Lett.* **84** 5987
[22] Ito K, Adachi J, Hall R, Motoki S, Shigemasa E, Soejima K and Yagishita A 2000 *J. Phys.* **33** 572
[23] Landers A, Weber T, Ali I, Cassimi A, Hattass M, Jagutzki O, Nauert A, Osipov T, Staudte A, Prior M H, Schmidt-Böcking H, Cocke C L, Dörner R *et al* 2001 *Phys. Rev. Lett.* **87** 013002
[24] Zare R 1972 *Molecular Photochem.* **4** 1
[25] McGuire J 1997 *Electron Correlation Dynamics in Atomic Collisions* (Cambridge: Cambridge University Press)
[26] Pavlychev A A 1999 *J. Phys.* **32** 2077
[27] Becker U 2000 Private Communication and invited talk on ICESS8
[28] Dörner R, Mergel V, Jagutzki O, Spielberger L, Ullrich J, Moshammer R and Schmidt-Böcking H 2000 *Phys. Rep.* **330** 96
[29] see Roentdek.com for details of the detectors
[30] Landers A *et al* to be published
[31] Lundqvist M, Edvardsson D, Baltzer P and Wannberg B 1996 *J. Phys. B: At. Mol. Opt. Phys.* **29** 1489
[32] Hsieh S and Eland J 1996 *J. Phys. B: At. Mol. Opt. Phys.* **29** 5795
[33] Lundqvist M, Baltzer P, Edvardsson D, Karlsson L and Wannberg B 1995 *Phys. Rev. Lett.* **75** 1058
[34] Dawber G, McConkey A, Avaldi L, MacDonald M, King G and Hall R 1994 *J. Phys.* **27** 2191
[35] Saito N, Heiser F, Hemmers O, Wieliczek K, Viefhaus J and Becker U 1996 *Phys. Rev.* A **54** 2004
[36] Hitchcock A, Lablanquie P, Morin P, Lizon E, Lugrin A, Simon M, Thiry P and Nenner I 1988 *Phys. Rev.* A **37** 2448
[37] Lablanquie P *et al* 1989 *Phys. Rev.* A **40** 5673
[38] Wetmore R, Le Roy R and Boyd R K 1984 *J. Phys. Chem.* **88** 6318
[39] Díez Muiño R, Rolles D, García de Abajo F J, Starrost F, Schattke W, Fadley C S and Van Hove M A 2001 *J. Electron Spectrosc. Relat. Phenom.* **99** 114
[40] Larsson M, Sundström L, Broström L and Mannervik S 1992 *J. Chem. Phys.* **97** 1750
[41] Mullin A S, Szavlarski D M, Yokoyama K, Gerber G and Lineberger W C 1992 *J. Chem. Phys.* **96** 3636